Turkish Journal of Electrical Engineering & Computer Sciences

http://journals.tubitak.gov.tr/elektrik/

Research Article

Turk J Elec Eng & Comp Sci
(2020) 28: 2433 – 2447

doi:10.3906/elk-1907-114

Reconfiguration-based hierarchical energy management in multimicrogrid systems considering power losses, reliability index, and voltage enhancement

Farid HAMZEH AGHDAM, **Navid TAGHIZADEGAN KALANTARI***, **Sajad NAJAFI RAVADANEGH**
Department of Electrical Engineering, Azarbaijan Shahid Madani University, Tabriz, Iran

Received: 15.07.2019 • **Accepted/Published Online:** 12.12.2019 • **Final Version:** 25.09.2020

Abstract: This paper presents a reconfiguration-based hierarchical energy management for interconnected microgrids known as multimicrogrid system. The goal is to minimize the operational costs of different entities alongside with finding the best topology to minimize the active power loss, enhance reliability index, and improve the voltage level. The distribution network (DN) includes several dispatchable and undispatchable distributed energy resources, energy storage devices, and multiple microgrids (MGs). The first layer of the optimization process is executed by each MG operator and each MG performs local energy management. Each MG operator informs the DN operator about its optimal schedules. Finally, global energy management with reconfiguration in the network topology is done by the DN operator. The energy management problem is modeled as a mixed-integer nonlinear programming problem. Simulations on a modified IEEE 33-bus distribution test system with multiple MGs is performed in GAMS environment.

Key words: Reconfiguration, multimicrogrid systems, energy management

1. Introduction

Nowadays electrical power systems are facing different issues such as increment in the electrical energy demand, growth of the greenhouse gases emissions, and security and reliability problems. A primitive solution for these problems is the expansion of existing generation and transmission systems, which seems to be infeasible due to its high costs. Another solution is utilizing renewable energy sources such as wind or PV systems as distributed energy resources (DERs), which may lead to many challenges for the DN operators. To overcome these challenges microgrids (MGs) are formed [1]. An MG is described as a cluster of the DERs (conventional or renewable), energy storage devices (ESDs), and loads [2, 3]. Energy management system is a vital tool in the MGs which aims to improve the efficiency i.e. extracting maximum available power from renewable energy resources (wind turbine, solar panel, etc.), deciding on the amount of produced power, performing demand response programs [4, 5], determining the policy of trading power with the upper stream network [3, 6–8], and choosing the best strategy for charging and discharging of the ESDs [9–11], and to top it all minimizing the costs.

The shaping of multiple MGs in the DN has led to the foundation of the multimicrogrid (MMG) systems in the DNs which may face challenges such as congestions or voltage stability due to their old infrastructures. Active reconfiguration of the DN is one possible solution to overcome the aforementioned issues. The configuration of the current DNs remains unchanged for long times. However, in smart DNs, the reconfiguration could be done much easier employing fast switches and modern communication infrastructures, and therefore it might be used

*Correspondence: taghizadegan@azaruniv.ac.ir

frequently. Thus, there have been many studies to investigate the feasibility of hourly reconfiguration [12–14].

The aim of the reconfiguration of the DN is to find a radial structure through changing the status of sectionalizers and tie switches to minimize the objective function. Usually, the objective function may contain minimizing the active power loss of the system, providing all the energy demanded, enhancing the voltage index and power quality, optimal switching under N-1 contingency, etc. [15–19]. It was first proposed by Merlin and Back intending to find the optimum topology to minimize the active power loss [20].

The DN reconfiguration problem is modeled as a mixed-integer nonlinear programming (MINLP) problem due to the nonlinear structure of power flow constraints and binary variables which determine the status of the switches. In the reviewed literature, optimization methods for solving the reconfiguration problem can be categorized into two main clusters: 1) mathematical techniques and 2) heuristic and metaheuristic methods. Dorostkar-Ghamsari et al. analyzed the feasibility of the hourly reconfiguration of the DN in the presence of renewable energy resources using mixed-integer second-order conic programming [15]. In this study, the effect of reconfiguration on the stability indices has been neglected and operational costs of DERs have not been considered. Authors in [21] proposed an approach based on mixed-integer programming (MIP) to formulate the reconfiguration problem of the DN for restoration after a fault occurs in the presence of ESDs; however, the penetration of renewable-based units was not taken into account. Others have applied heuristic and metaheuristic methods to the reconfiguration problem of the DN. Authors in [22] investigated the impacts of DERs on the reconfiguration of the DN, considering the voltage stability in the optimization problem utilizing a Pareto-based metaheuristic optimization algorithm. In this study, the operational costs of different units in the system have been omitted and there is no battery storage system. Dahalan et al. [23] proposed a simultaneous method for identifying the optimal DN reconfiguration and DERs utilizing evolutionary algorithms. The biggest flaws of this study are that the cost of switching in the reconfiguration process and the presence of renewable-based units have been neglected. Moreover, a reconfiguration methodology for the DN using cuckoo search algorithm has been suggested in [24] with aiming at minimizing active power loss and enhancing the voltage stability. In this study, the focus is on the evolutionary algorithm without any attention to the system operation. It is obvious in the research in the field of reconfiguration is that the development of DN and considering more penetration of MGs in the system is lacking.

As mentioned earlier, MMG-based DNs are of interest to the researchers. Many researchers have studied the energy management in such systems. Authors in [25] suggested an approach for optimal power dispatch of MMG systems considering network uncertainties. The proposed method is a momentary power dispatch without contemplating the effect of time and energy storages in the operational costs. In [26], stochastic energy management for an MMG system in presence of clean productions has been proposed. The effect of the presence of microgrids on the stability and reliability indices of the system has not been evaluated. Authors in [27] presented a decentralized-based Markov decision process intending to minimize the MGs operational costs. It is noteworthy to mention that the authors did not consider network constraints and MGs are controlled by the DN operator. Authors in [28] suggested an energy management strategy named nested EMS for scheduling of MMG system. Although the authors did a perfect job in the field of energy management of MMG systems, it might be better to consider security constraints and stability indices in the process. Moreover, authors in [29] investigated the impact of congestion in the lines of the MMG system in the energy management procedure. In this study, the probability of contingencies is calculated according to the amount of power passage through the respective line. To sum it up, in all the mentioned literature of MMG systems, the structure of the system has been fixed and the possibility of changing the shape has been neglected.

In the energy management process due to the goal of the MGs in MMG systems, they try to maximize their benefit by energy transactions with the upper network, which may cause many issues for the distribution system that might be solved by reshaping the topology of the system. Thus, in this paper, a hierarchical energy management system for an active DN consisting of local DERs, ESDs, and MMGs, considering reconfiguration model is presented. The process contains two steps and in the first step, local energy management is done in each MG to determine the schedules of its entities. In the second step, the DN operator performs global energy management using the data gathered from the local energy management of the MGs and tries to find the best structure for the DN by reconfiguration. The problem is modeled as a multiobjective mixed-integer nonlinear programming (MINLP) aiming at minimizing power losses and energy not supplied (ENS) as the reliability index and also enhancing voltage stability. The reconfiguration is done in a way that the topology of the DN remains radial. This is because of many benefits such as plainness of analysis and coordination, low operational cost, and decreasing the short circuit current. To sum it up, the main contributions of this study are as follows:

- Proposing a novel reconfiguration-based hierarchical energy management (RBHEMS) system for an active DN with MMGs, DERs, and ESDs.
- Modelling the energy management problem as a multiobjective optimization problem.
- Considering an MINLP-based optimization for the DN reconfiguration-based energy management.
- Analyzing the behavior of the proposed method under contingencies and abnormal conditions.
- Considering the effect of changing coefficients of power loss and reliability index in the objective function.

The rest of the article is sectionalized as follows: In section 2, modeling and mathematical formulations of each unit are discussed. The recommended framework for RBHEMS is presented in section 3. Section 4 is dedicated to simulations and examining of the proposed method on a test system. The final section includes the conclusion of the paper.

2. Mathematical Modelling of the System

An active DN with the capability of reconfiguration, consisting of various MGs, dispatchable DERs, wind turbines, PVs, batteries as ESDs and loads, is used in this paper to evaluate the effectiveness of the proposed method. The system structure is shown in Figure 1 which consists of three MGs alongside other entities. Moreover, each MG has dispatchable DERs, undispatchable units such as PV systems and wind turbines, ESDs, and loads. The following is the detailed modeling of the units.

2.1. MMG-based DN structure

The structure of the MMG-based test system is depicted in Figure 2 which is a modified version of the IEEE 33-bus test system. There are some normally open and normally closed switches which are in such status that keep the DN operate in radial form. which are in such status that keep the DN operate in radial form. The DN operator is responsible to perform the switching actions besides the energy management and power transactions with MGs and upper grid. The operations of the entities of each MG such as DERs, batteries, and also deciding about energy trading are controlled by its local controller.

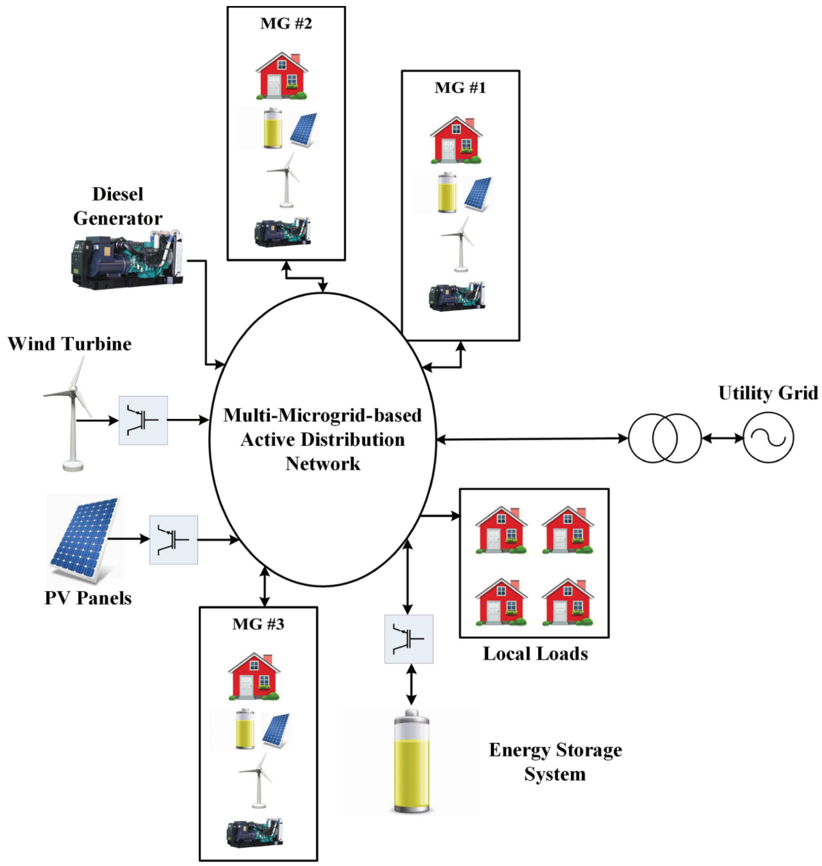

Figure 1. MMG system structure.

2.2. Dispatchable units

Units with the capability of controlling their output power are considered dispatchable generation units i.e. diesel generators, fuel cells, etc. In this article, a diesel generator is assumed as the dispatchable system which has the following constraints for its operation.

$$0 \leq P_g(t) \leq \vartheta_g(t).P_{g,\max},\ \vartheta_g(t) \in \{0,1\} \tag{1}$$

$$|P_g(t) - P_g(t-1)| \leq ramp_g \cdot P_{g,\max} \tag{2}$$

$$P_g^2(t) + Q_g^2(t) \leq S_{g,\max}^2 \tag{3}$$

Equation (1) stands for the generation limit of the diesel generator. $P_g(t)$ is the active power generated by the generator, g, and ϑ_g is a binary variable which determines the on/off status of the generator and Equation (2) shows its ramp rate constraints where P_g^{Max} is maximum capacity of the generator and $ramp_g$ is its ramp rate. In order to contemplate complex power constraint of the diesel generator, Equation (3) is considered in the modeling. Q_g and $S_{g,\max}$ are the generated reactive power and complex power capacity.

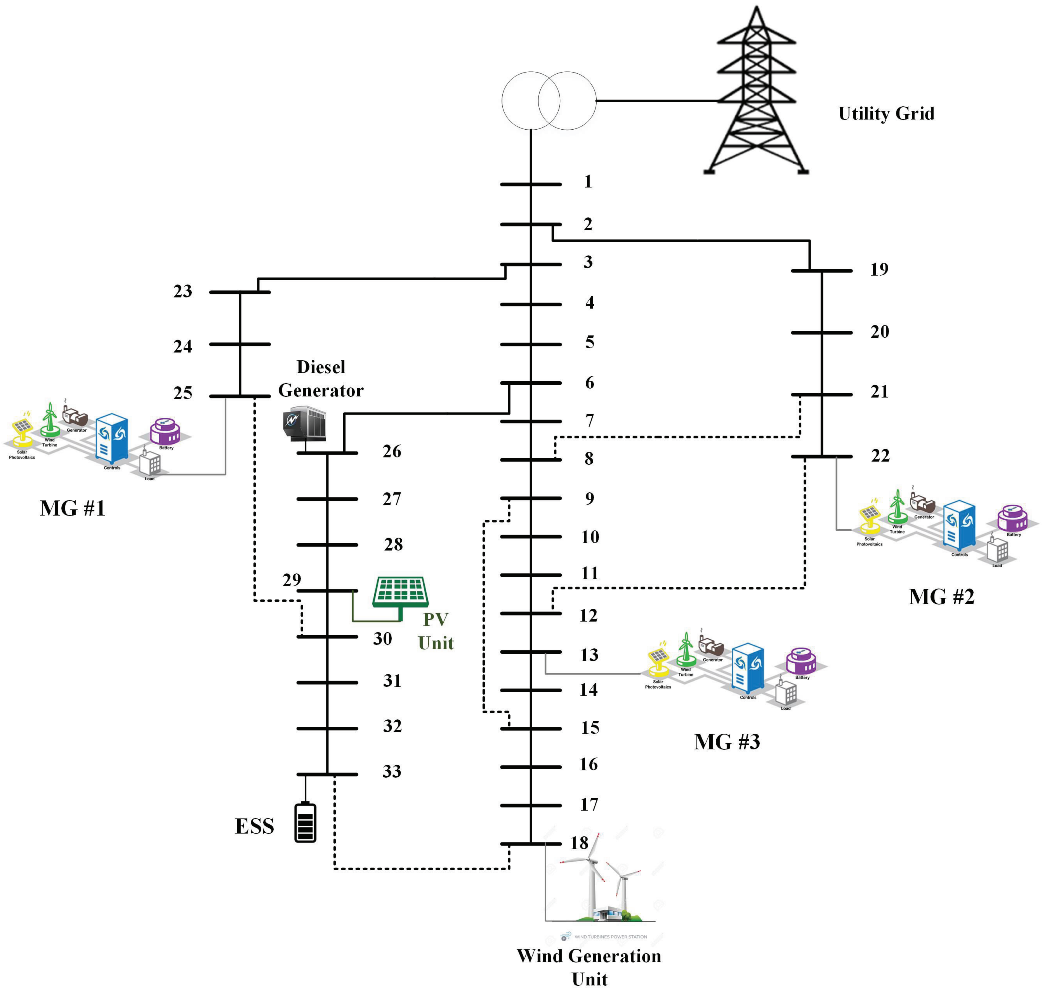

Figure 2. Modified IEEE 33-bus test system containing multiple MGs, DERs, and ESD.

The operational cost of a diesel generator is usually considered as a quadratic function of its produced power as shown in Equation (4). Moreover, to avoid frequent variations in its status, usually a start-up cost is taken into account which could be presented using Equations (5) and (6) [30]:

$$C_{op,g}(P_g(t)) = \alpha_g \cdot P_g^2(t) + \beta_g \cdot P_g(t) + c_g \tag{4}$$

$$C_{st,g}(t) = \chi_g(t) \times {C_g}^{SU} \tag{5}$$

$$\chi_g(t) = \max\{(\vartheta_g(t) - \vartheta_g(t-1), 0)\} \tag{6}$$

In above equations, α_g, β_g, and c_g are constants representing the cost function coefficients of generator, g. Moreover, ϑ_g is an ancillary binary variable indicating changes in its on/off status.

2.3. Undispatchable generators

PV generation units and wind turbines which have stochastic output power depending on the weather are considered as undispatchable units. The generated power in such systems is dependent on the environmental circumstances i.e. wind velocity, temperature, and solar radiation. This leads to the entrance of uncertainty to the system. In this study, the PV system and wind turbine are considered in the structure of the MMG system. Usually, to model the uncertainty, probability distribution function (PDF) for the stochastic variables are used.

The PV generation is occupied with solar irradiance which follows a lognormal PDF. The respective relationships are illustrated in terms of Equations (7) and (8). In these equations, H is the amount of solar irradiance with the mean of μ_H and variance σ_H^2. H_{std} and H_{std} are respective representatives standard and certain values of solar irradiance. Moreover, P_{PV} and $P_{PV,R}$ stand for the output and the rated power of the PV unit, respectively.

$$f_H(H) = \frac{1}{H \cdot \sqrt{2\pi\sigma_H^2}} exp[\frac{-(\ln H - \mu_H)^2}{2\sigma_H^2}] \quad H \geq 0 \tag{7}$$

$$P_{PV} = \begin{cases} P_{PV,R} \times (\frac{H^2}{H_{std} \cdot H_{cer}}) & H \leq H_{cer} \\ P_{PV,R} \times (\frac{H^2}{H_{std}}) & H_{cer} \leq H \end{cases} \tag{8}$$

Another source of stochastic energy in electrical power systems is wind energy. Wind turbines are responsible for converting the kinetic energy of wind into electrical energy. The wind velocity is the main factor for achieving the energy which is usually modeled with Weibull PDF. The relations for Weibull PDF of the wind and output power of wind turbine as a function of wind velocity is shown in Equations (9) and (10). In these equations, P_{WT} and $P_{WT,R}$ show the output and rated power of the wind turbine. Moreover, V, V_R, V_{C-I}, and V_{C-O} are respective representatives for wind velocity, rated, cut-in and cut-out speed values of the wind turbine. Besides, α and β are symbols for shape and scale factors of the Weibull PDF.

$$f_V(V) = (\frac{\alpha}{\beta})(\frac{V}{\beta})^{\alpha-1} \exp[-(\frac{V}{\beta})^{\alpha}] \quad 0 \leq V \leq \infty \tag{9}$$

$$P_{WT} = \begin{cases} 0 & V \leq V_{C-I}, \quad V \geq V_{C-O} \\ \frac{V - V_{C-I}}{V_R - V_{C-I}} P_{WT,R} & V_{C-I} \leq V \leq V_R \\ P_{WT,R} & V_R \leq V \leq V_{C-O} \end{cases} \tag{10}$$

2.4. Energy storage devices (ESD)

In this paper, batteries are considered as the ESD. Equations (11)–(19) show the constraints of the battery system. Maximum charging and discharging limits of the battery are presented in the form of Equations (11) and (12). In these equations, $P_{bat,ch}$ and $P_{bat,disch}$ show the charging and discharging power of the battery and $P_{bat,\max}$ stands for the maximum allowable power flow from the battery system. Moreover, $\vartheta_{bat,ch}$ and $\vartheta_{bat,disch}$ are binary variables illustrating battery charging or discharging status which should not be equal to 1 at the same time to avoid simultaneous charging and discharging that is accomplished by means of Equation (13). Equations (14)–(17) illustrate the constraints for state of charge (SoC) of the battery system. Furthermore, Equations (18) and (19) stand for the complex power limitation of the system. S_{bat} is apparent power of the battery and which is equal to active power of the battery.

$$0 \leq P_{bat,ch}(t) \leq \vartheta_{bat,ch}(t) \cdot P_{bat,\max} \tag{11}$$

$$0 \leq P_{bat,disch}(t) \leq \vartheta_{bat,disch}(t) \cdot P_{bat,\max} \tag{12}$$

$$\vartheta_{bat,ch}(t) + \vartheta_{bat,disch}(t) \leq 1,\ \ \vartheta_{bat,ch}(t), \vartheta_{bat,disch}(t) \in \{0,1\} \tag{13}$$

$$SoC_{bat}(t) = SoC_{bat}(t-1) - \frac{1}{P_{bat,\max}} \cdot (P_{bat,disch}(t) - P_{bat,ch}(t)) \tag{14}$$

$$0 \leq SoC_{bat}(t) \leq 1 \tag{15}$$

$$SoC_{bat}(t_0) = SoC_{bat,init} \tag{16}$$

$$SoC_{bat}(t_{23}) = SoC_{bat,final} \tag{17}$$

$$P_{bat}(t) = P_{bat,ch}(t) - P_{bat,disch}(t) \tag{18}$$

$$P_{bat}^2(t) = S_{bat}^2(t) \tag{19}$$

3. Problem formulation

In this section, models for RBHEMS are developed for the studied system. In operation of the MGs, due to variations of electricity price and probabilistic output power of renewable energy-based DERs, the concept of shortage or surplus power, is presented with the aim of selling the surplus power to the upper grid and buying the shortage power from the DN. In the first step of the RBHEMS, each MG controller carries out energy management in order to determine its schedules i.e. surplus power, shortage power, the output power of the dispatchable DERs, and battery charging or discharging status. In the second step, the DN operator performs a global optimization based on the collected data of the MGs. It tries to specify the output schedules of its independent local entities and the status of the tie line keys to reduce total power loss and enhance the voltage index. In case of contingencies in one of its lines, again it tries to find the best topology to keep the DN in the radial structure and supply the loads without any interruptions. Figure 3 demonstrates the procedure of the optimization process. Furthermore, the following contains the mathematical formulations for the RBHEMS process.

3.1. First step: MG local energy management

MGs consist of dispatchable or undispatchable DERs i.e. diesel generators, wind turbines, PV systems, etc. MG operator is responsible for the optimization of its local entities and determining their duties.

The goal of this step for each MG is to minimize its operational cost which can be expressed in terms of Equation (20). In the objective function the first term is dedicated to the operational cost of respective diesel generator and second term illustrates the cost of power transactions with the DN where $price_{buy,DN}(t)$ and

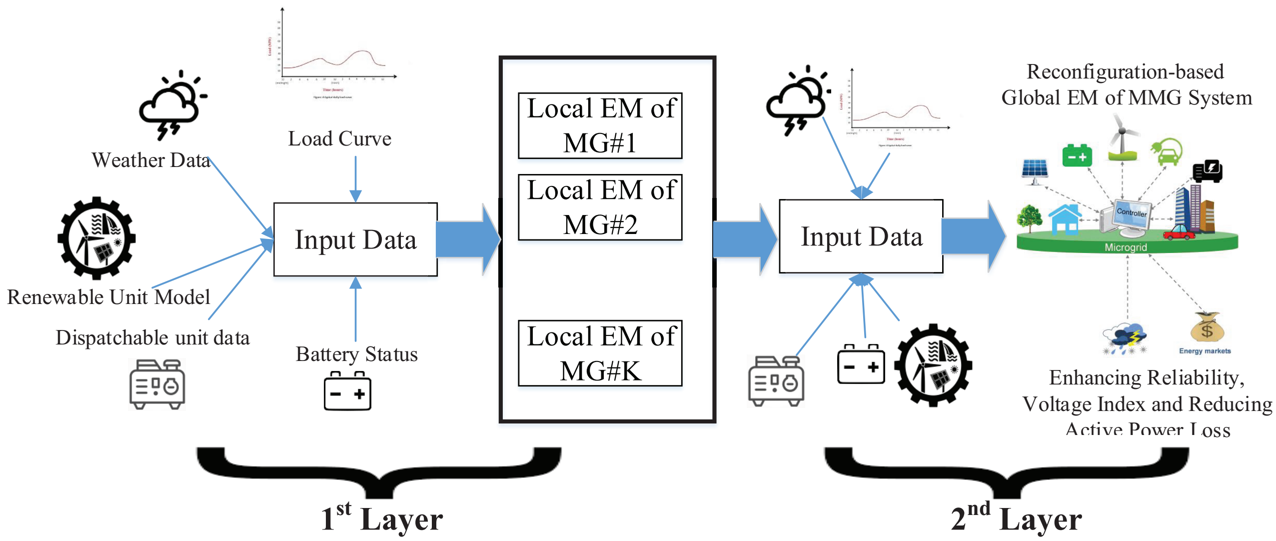

Figure 3. Steps of RBHEMS in MMG system.

$price_{sell,DN}(t)$ are energy prices in the DN for purchasing and selling electricity. Moreover, $P_{shortage}(t)$ and $P_{surplus}(t)$ stand for power shortage and surplus. In order to contemplate the impact of uncertainties, scenarios for the generation of the PV, and wind systems are considered. p_s determines the probability of scenario s. Monte Carlo Simulation (MCS) is employed to generate different scenarios for each uncertain source which is a very suitable approach in problems involving different uncertain sources [31]. The generation of the scenarios has been performed independently and the correlation among the stochastic variables has been neglected. In order to reduce the burden of calculations, fast forward selection as the scenario reduction method has been employed [32].

$$\begin{aligned}\min\ \text{O.F.} \quad = \quad & \sum_t \left\{ \sum_s p_s \times \left(\sum_g [C_{op}(P_{g,s}(t)) + C_{st,g,s}(t)] \right.\right. \\ & \left.\left. + price_{buy,DN}(t) \cdot P_{shortage,s}(t) - price_{sell,DN}(t) \cdot P_{surplus,s}(t) \right) \right\} \end{aligned} \tag{20}$$

$$subject\ to: \ Equations\ (1) - (19) \quad \forall s$$

$$P_{g,s}(t) + P_{WT,s}(t) + P_{PV,s}(t) - P_{load}(t) - P_{surplus,s}(t) + P_{shortage,s}(t) = 0 \tag{21}$$

3.2. Second step: reconfiguaration-based global energy management

In the second step, the DN operator starts the global optimization according to the gathered data of the MGs and lines with contingency or faulty conditions. The objective function in this stage is similar to Equation (20); however, due to the capability of reconfiguration, the DN operator tries to find the best topology for the DN to reduce active power loss, enhancing voltage stability and improving reliability index. This reconfiguration is done according to the expected values gained from various objectives in different scenarios. Besides, it is assumed that in the DN, bus 1 has a voltage amplitude of 1 p.u. and power transactions with the utility grid is done through this bus. Equation (22) illustrates the objective function of this stage which consists of two main terms. The first term refers to the switching cost and the second term is an expected cost which contains multiple objectives as operational costs of local DERs, reliability, and voltage indices. Moreover, to make the calculations more realistic, the power flow constraints have been considered in terms of Equations (23)–(32) [33, 34].

$$\min \sum_{t} \left\{ \sum_{NormallyOpen} \lambda_{i,j,t} \cdot C_{Switch} + \sum_{NormallyClose} (1-\lambda_{i,j,t}) \cdot C_{Switch} + \right.$$
$$\sum_{s} p_s \times [\sum_{g} [C_{op}(P_{g,DN,s}(t)) + C_{st,g,DN,s}(t)] + [price_{buy,utility}(t) \cdot P_{buy,DN,s}(t) - price_{sell,utility}(t) \cdot] \tag{22}$$
$$P_{sell,DN,s}(t) + \sum_{\xi} [price_{sell,DN}(t) \cdot P_{surplus,\xi,s}(t) - price_{buy,DN}(t) \cdot P_{shortage,\xi,s}(t)] +$$
$$\left. price_{buy,utility}(t) \cdot P_{loss,s}(t) + price_{Shame} \cdot ENS_s(t) + \sum_{i} \Delta U_{i,s}(t)] \right\}$$

$$subject\ to: \ Equations\ (1)-(19),(21) \quad \forall s$$

$$\Delta U_{i,s}(t) = \left[\frac{U_1(t) - U_{i,s}(t)}{U_1(t)} \right]^2 \tag{23}$$

$$S_{net,i,s}(t) = S_{bat,i,s}(t) + S_{load,i}(t) - S_{g,i,s}(t) \tag{24}$$

$$P_{net,j,s}(t) = P_{i,j,s}(t) - R_{i,j} \cdot I^2_{i,j,s} - \sum P_{j,q,s}(t) \tag{25}$$

$$Q_{net,j,s}(t) = Q_{i,j,s}(t) - X_{i,j} \cdot I^2_{i,j,s} - \sum Q_{j,q,s}(t) \tag{26}$$

$$U^2_{i,s}(t) - 2 \times [R_{i,j} \cdot P_{i,j,s}(t) \ + \ X_{i,j} \cdot Q_{i,j,s}(t)] + (R^2_{i,j} + X^2_{i,j}) \cdot I^2_{i,j,s}(t) - U^2_{j,s}(t) + U^2_{i,j,s}(t) = 0 \tag{27}$$

$$U_{\min} \le U_{i,s}(t) \le U_{Max} \tag{28}$$

$$-U^2_{i,j,\max} \cdot (1-\lambda_{ij}) \le U^2_{i,j,s}(t) \le U^2_{i,j,\max} \cdot (1-\lambda_{ij}) \tag{29}$$

$$I^2_{i,j,s}(t) = \frac{S^2_{i,j,s}(t)}{U^2_{i,s}(t)} \tag{30}$$

$$0 \le I^2_{i,j,s}(t) \le I^2_{i,j,max} \cdot \lambda_{ij} \tag{31}$$

$$\sum_{ij \in Loop\ K} \lambda_{ij} \leq N_K - 1 \tag{32}$$

$R_{i,j}$ and $X_{i,j}$ are respective representatives for resistance and reactance of the line between buses i and j. Furthermore, the current flowing through line ij and its voltage drop is shown by $I_{i,j}$ and $U_{i,j}$. Moreover, U_i, $S_i(t)$, $S_{bat,i}(t)$, $S_{load,i}(t)$, and $S_{g,i}(t)$ stand for voltage, net apparent power, apparent power of battery, load, and generator of bus i, respectively. The apparent power itself consists of real and imaginary parts as P_i and Q_i. Active and reactive power passing through the link ij are $P_{i,j}$ and $Q_{i,j}$, respectively. λ_{ij} is a binary variable that indicates the status of the switch in the link ij. Presence of λ makes the problem a mixed integer programming. Furthermore, presence of nonlinear constraints in the problem, leads to a MINLP problem. Also C_{Switch} and $price^{Shame}$ are the cost of the switching and the price of the shame for the interrupted load, respectively. ΔU is the voltage deviation index and is expressed in terms of Equation (23). Equation (24) indicates the net complex power injected to bus $\#i$. Equations (25) and (26) illustrate the steady-state active and reactive power flows. Equation (27) demonstrates the relationship between the voltages of two nodes and the power flow through their respective line, in which $U_{i,j}$ is a supplementary variable indicating the voltage drop according to switching actions and system topology which is zero in case of closed switches as in Equation (29) and otherwise has an adequate amount. Voltage constraint is brought in Equation (28) and finally current limits according to the status of the switches is shown in Equation (31). The configuration of the DN should remain radial which is guaranteed through Equation (32). This equation indicates that the number of the closed lines in any loop should be smaller than the total number of the lines in that specific loop. In other words, it means that by opening at least one switch in each loop, the radial structure of the DN would be assured [21].

4. Simulations

In this section, the proposed RBHEMS' mathematical implementation and computational results are demonstrated in an IEEE 33-bus distribution test system modified with three microgrids and some local DERs which is depicted in Figure 2. To examine the RBHEMS, solver BARON in GAMS software is used. MGs #1 and #2 contain PV generation units, wind turbines, dispatchable DERs. The third MG, have no dispatchable DER and the only generation units are a wind turbine and PV system alongside the ESD. Parameters of the diesel generators and the batteries of each MG and the DN of the test system are illustrated in Table 1. Figure 4 shows the hourly energy pricing in the DN.

Using the aforementioned data, the results of the local optimization of the MGs are illustrated in Figure 5.

Table 1. Generator and energy storage parameters.

Parameter	α ($$/MW^2$)	β ($$/MW$)	l ($)	Gen. cap (MW)	St. up cost ($)	Ramp up (MW/h)	Bat. cap (MWh)	Init. energy (MWh)	Fin. energy (MWh)	Conv. cap. (KW)	Conv. eff. (%)
MG1	18	90	0	2.1	200	0.3	1	0.2	0.5	500	98
MG2	15	85	0	1.6	200	0.3	1	0.2	0.5	500	98
MG3	-	-	-	-	-	-	1	0.2	0.5	500	98
DN	12	75	0	3	150	0.2	3	1.2	1	750	99

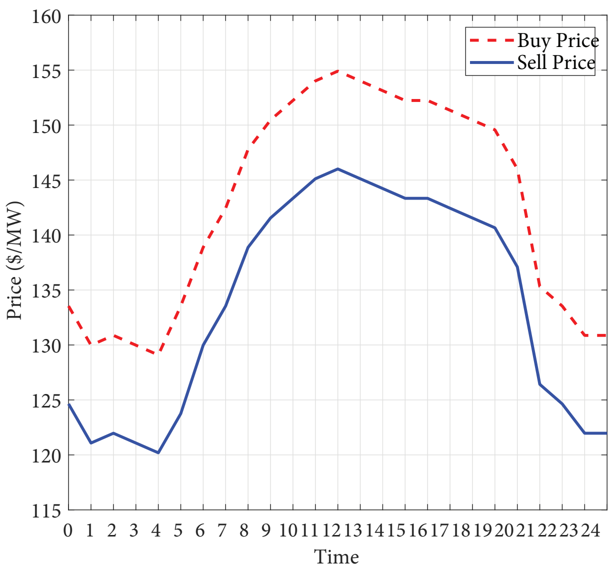

Figure 4. Hourly energy price.

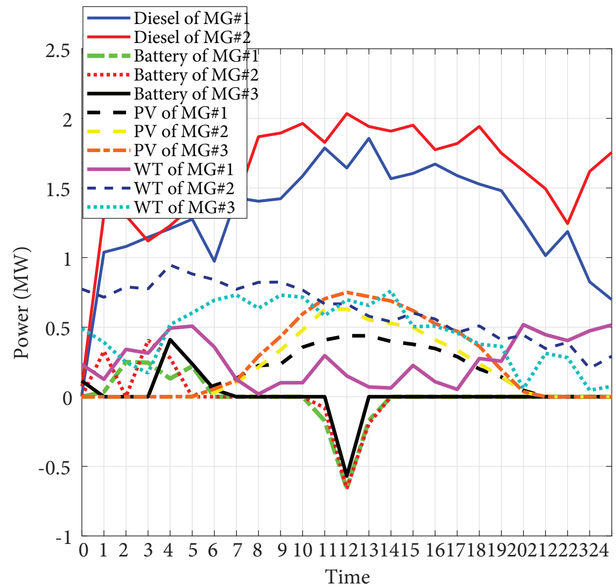

Figure 5. Local Energy Management of the MGs.

Using local optimization results, the DN operator gathers the output schedules of the MGs and gets ready to start the RBHEMS to determine the optimum hourly switching strategy and the best topology to minimize operational cost and power loss beside enhancing the voltage stability. However, giving different coefficients to costs of reliability index and power loss in the main objective function may lead to different results. For instance, reducing the ENS leads to more power loss which might be due to the load shedding and reducing the power flow in some lines. Accordingly, a trade-off must be done between the coefficients of the active power loss and the reliability terms in the objective function. Table 2 demonstrates the amount of the active power loss and the reliability index, according to their coefficients in the objective function. The best point occurs when 0.4 is given to the power loss and 0.6 is assigned to the ENS.

Table 2. Effect of changing the coefficients of power loss and ENS in the objective function.

Power loss coefficient	Total energy loss (MWh)	Reliability index coefficient	ENS (MWh)
0.9	0.895	0.1	0.205
0.8	0.881	0.2	0.218
0.7	0.866	0.3	0.235
0.6	0.816	0.4	0.266
0.5	0.801	0.5	0.362
0.4	0.792	0.6	0.509
0.3	0.785	0.7	0.651
0.2	0.781	0.8	0.822
0.1	0.779	0.9	1.013

Selecting convenient values for the coefficients of power loss and ENS, the RBHEMS begins. Figure 6 shows the output schedules of local entities of the DN in this layer. Moreover, the expected power loss reduction in the RBHEMS process in comparison with HEMS without reconfiguration is demonstrated in Figure 7. It is assumed that there is a contingency in the line connecting busses 2 and 3 between hours 20 to 22. Accordingly, due to load loss, in the system without reconfiguration, the power loss in this period is less than that in the system with reconfiguration capability. In the other hours, reconfiguration has reduced the power loss. The RBHEMS has reduced the total energy loss of the system from 0.9 MWh to 0.816 MWh.

The expected costs for the DN, MG1, MG2, and MG3 have become $8274, $2833, $1712, and $–962, respectively. Also in Figure 8, enhancement in the expected voltage of the busses at hour 18, considering the voltage stability index in the objective function, is shown.

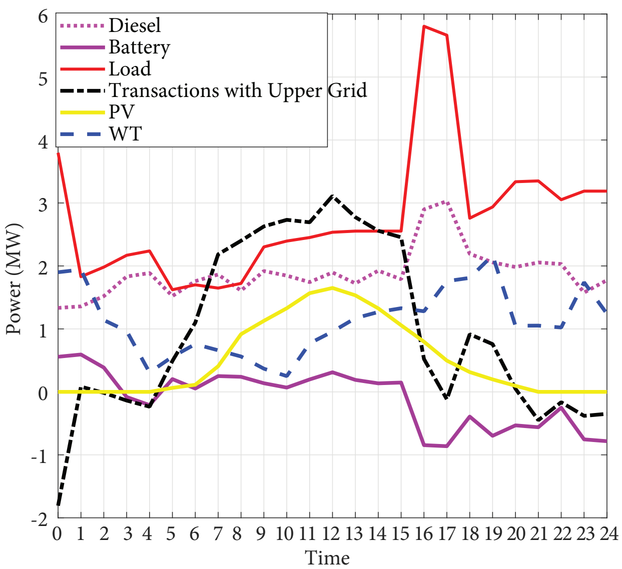

Figure 6. Output schedules of various entities.

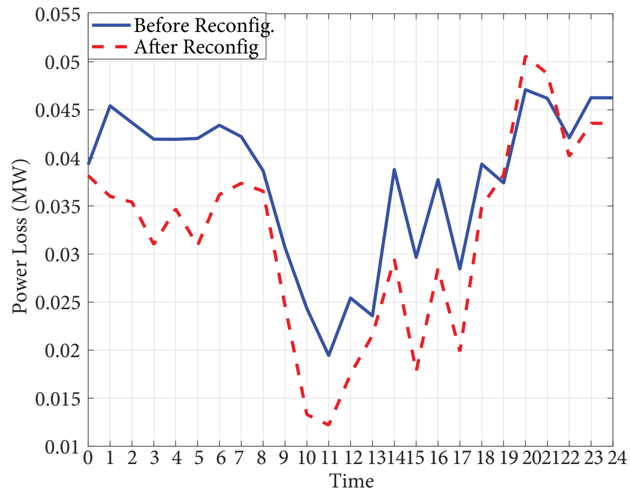

Figure 7. Active power loss before and after reconfiguration.

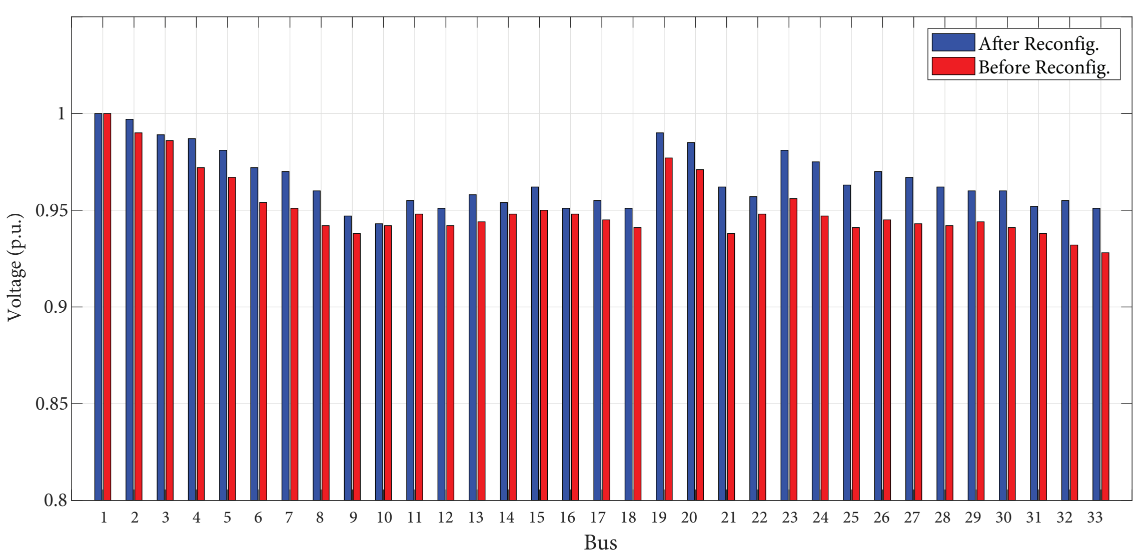

Figure 8. Voltage enhancement in the busses at hour 18.

The status of the switches for different hours is tabulated in Table 3. The ENS before and after the reconfiguration is also illustrated in Table 4, which also proves the effectiveness of the proposed method. It is obvious that without reconfiguration, the value of the ENS is more than of that when performing reconfiguration. The total ENS values before and after reconfiguration are 4.1 MWh and 0.27 MWh, respectively. The higher ENS before reconfiguration, between hours 20 to 22, is a result of contingency which also indicates that in the case of failure in the lines, reconfiguration helps to overcome the event.

Table 3. Reconfiguration results.

t	Open switches	t	Open switches
T0	10-11, 9-15, 8-21, 18-33, 25-29	T12	10-11, 12-22, 8-21, 18-33, 25-30
T1	10-11, 9-15, 8-21, 18-33, 25-29	T13	10-11, 12-22, 8-21, 18-33, 25-30
T2	10-11, 9-15, 8-21, 18-33, 25-29	T14	10-11, 12-22, 8-21, 18-33, 25-30
T3	10-11, 9-15, 8-21, 18-33, 25-29	T15	10-11, 12-22, 8-21, 18-33, 25-30
T4	10-11, 9-15, 8-21, 18-33, 25-29	T16	10-11, 12-22, 8-21, 18-33, 25-30
T5	10-11, 9-15, 8-21, 18-33, 25-29	T17	10-11, 12-22, 8-21, 18-33, 25-30
T6	10-11, 9-15, 8-21, 18-33, 25-29	T18	10-11, 12-22, 8-21, 18-33, 25-30
T7	10-11, 9-15, 8-21, 18-33, 25-29	T19	10-11, 12-22, 8-21, 18-33, 25-30
T8	10-11, 9-15, 8-21, 18-33, 25-29	T20	2-3, 10-11, 12-22, 15-16, 25-30
T9	10-11, 9-15, 8-21, 18-33, 25-29	T21	2-3, 10-11, 12-22, 15-16, 25-30
T10	10-11, 12-22, 8-21, 18-33, 25-30	T22	2-3, 10-11, 12-22, 15-16, 25-30
T11	10-11, 12-22, 8-21, 18-33, 25-30	T23	2-3, 10-11, 12-22, 15-16, 25-30

Table 4. Expected ENS before and after reconfiguration.

t	T0	T1	T2	T3	T4	T5	T6	T7	T8	T9	T10	T11
Before Reconfig	0	0	0	0	0	0	0	0	0	0	0	0
After Reconfig	0	0	0	0	0	0	0	0	0	0	0	0
t	T12	T13	T14	T15	T16	T17	T18	T19	T20	T21	T22	T23
Before Reconfig	0.046	0.118	0.027	0.102	0.384	0.246	0.308	0.489	0.743	0.783	0.495	0.372
After Reconfig	0.009	0.013	0.013	0.089	0.016	0.015	0.016	0.017	0.026	0.023	0.013	0.016

5. Conclusion

In this paper, a reconfiguration-based hierarchical energy management system for a multimicrogrid-based distribution network has been proposed. The goal of the optimization process is to reduce the operational costs and simultaneously find the best topology to enhance the voltage stability index, reduce active power loss, and improve the reliability index. In the first layer, each MG operator solves a local energy management problem to determine the schedule of its units and delivers its information to the distribution network operator. The distribution network operator performs global energy management besides a reconfiguration. Finally, simulations in a modified version of the IEEE distribution test system which show the effectiveness of the proposed method are done.

References

[1] Hagh MT, Aghdam FH. Smart hybrid nanogrids using modular multiport power electronic interface. In: 2016 IEEE Innovative Smart Grid Technologies-Asia (ISGT-Asia); Melbourne, VIC, Australia; 2016. pp. 618-623.

[2] Hatziargyriou N. Microgrids: Architectures and Control. USA: John Wiley & Sons; 2014.

[3] Chaouachi A, Kamel RM, Andoulsi R, Nagasaka K. Multiobjective intelligent energy management for a microgrid. IEEE Transaction on Industrial Electronics 2013; 60(4): 1688-1699.

[4] Wang Z, Gu C, Li F, Bale P, Sun H. Active demand response using shared energy storage for household energy management. IEEE Transactions on Smart Grid 2013; 4(4): 1888-1897.

[5] Bui VH, Hussain A, Kim HM. A multiagent-based hierarchical energy management strategy for multimicrogrids considering adjustable power and demand response. IEEE Transaction on Smart Grid 2018; 9(2): 1323-1333.

[6] Jiang Q, Xue M, Geng G. Energy management of microgrid in grid-connected and stand-alone modes. IEEE Transactions on Power Systems; 2013; 28(3): 3380-3389.

[7] Korkas CD, Baldi S, Michailidis I, Kosmatopoulos EB. Intelligent energy and thermal comfort management in grid-connected microgrids with heterogeneous occupancy schedule. Applied Energy 2015; 149: 194-203.

[8] Gabbar HA, Abdelsalam AA. Microgrid energy management in grid-connected and islanding modes based on SVC. Energy Conversion and Management 2014; 86: 964-972.

[9] Rahbar K, Xu J, Zhang R. Real-time energy storage management for renewable integration in microgrid: An off-line optimization approach. IEEE Transactions on Smart Grid 2015; 6(1): 124-134.

[10] Mohammadi S, Soleymani S, Mozafari B. Scenario-based stochastic operation management of microgrid including wind, photovoltaic, micro-turbine, fuel cell and energy storage devices. International Journal of Electrical Power & Energy Systems 2014; 54: 525-535.

[11] Liu N, Chen Q, Lu X, Liu J, Zhang J. A charging strategy for PV-based battery switch stations considering service availability and self-consumption of PV energy. IEEE Transactions on Industrial Electronics 2015; 62(8): 4878-4889.

[12] Othman AM, El-Fergany AA, Abdelaziz AY. Optimal reconfiguration comprising voltage stability aspect using enhanced binary particle swarm optimization algorithm. Electric Power Components and Systems 2015; 43(14): 1656-1666.

[13] Imran AM, Kowsalya M, Kothari DP. A novel integration technique for optimal network reconfiguration and distributed generation placement in power distribution networks. International Journal of Electrical Power & Energy Systems 2014; 63: 461-472.

[14] Imran AM, Kowsalya M. A new power system reconfiguration scheme for power loss minimization and voltage profile enhancement using fireworks algorithm. International Journal of Electrical Power & Energy Systems 2014; 62: 312-322.

[15] Dorostkar-Ghamsari MR, Fotuhi-Firuzabad M, Lehtonen M, Safdarian A. Value of distribution network reconfiguration in presence of renewable energy resources. IEEE Transaction on Power Systems 2016; 31(3): 1879-1888.

[16] Kashem MA, Ganapathy V, Jasmon GB. Network reconfiguration for load balancing in distribution networks. IEE Proceedings-Generation, Transmission and Distribution 1999; 146(6): 563-567.

[17] Coelho A, Rodrigues AB, Da Silva MG. Distribution network reconfiguration with reliability constraints. In: International Conference on Power System Technology; Singapore, Singapore; 2004. pp. 1600-1606.

[18] Hedman KW, Ferris MC, O'Neill RP, Fisher EB, Oren SS. Co-optimization of generation unit commitment and transmission switching with N-1 reliability. IEEE Transactions on Power Systems 2010; 25(2): 1052-1063.

[19] Aghdam FH, Salehi J, Ghaemi S. Contingency based energy management of multimicrogrid based distribution network. Sustainable Cities and Society 2018; 41: 265-274.

[20] Merlin A. Search for a minimal-loss operating spanning tree configuration for an urban power distribution system. In: Proceedings of 5th PSCC; Cambridge, England; 1975. pp. 1-8.

[21] Moradzadeh B, Tomsovic K. Mixed integer programming-based reconfiguration of a distribution system with battery storage. In: North American Power Symposium (NAPS); Champaign, IL, USA; 2012. pp. 1-6.

[22] Asrari A, Wu T, Lotfifard S. The impacts of distributed energy sources on distribution network reconfiguration. IEEE Transactions on Energy Conversion 2016; 31(2): 606-613.

[23] Mohd Dahalan W, Mokhlis H, Ahmad R, Abu Bakar AH, Musirin I. Simultaneous network reconfiguration and DG using EP method. International Transactions on Electrical Energy Systems 2015; 25(11): 2577-2594.

[24] Nguyen TT, Truong AV. Distribution network reconfiguration for power loss minimization and voltage profile improvement using cuckoo search algorithm. International Journal of Electrical Power & Energy Systems 2015; 68: 233-242.

[25] Nikmehr N, Najafi Ravadanegh S. A study on optimal power sharing in interconnected microgrids under uncertainty. International Transactions on Electrical Energy Systems 2016; 26(1): 208-232.

[26] Aghdam FH, Ghaemi S, Kalantari NT. Evaluation of loss minimization on the energy management of multimicrogrid based smart distribution network in the presence of emission constraints and clean productions. Journal of Cleaner Production 2018; 196: 185-201.

[27] Wu J, Guan X. Coordinated multimicrogrids optimal control algorithm for smart distribution management system. IEEE Transactions on Smart Grid 2013; 4(4): 2174-2181.

[28] Hussain A, Bui VH, Kim HM. A resilient and privacy-preserving energy management strategy for networked microgrids. IEEE Transactions on Smart Grid 2018; 9(3): 2127-2139.

[29] Aghdam FH, Salehi J, Ghaemi S. Assessment of power flow constraints impact on the energy management system of multimicrogrid based distribution network. Journal of Energy Management and Technology 2018; 2(3): 31-41.

[30] Aghdam FH, Hagh MT. Security Constrained Unit Commitment (SCUC) formulation and its solving with Modified Imperialist Competitive Algorithm (MICA). Journal of King Saud University-Engineering Sciences 2019; 31(3): 253:261.

[31] Aien M, Rashidinejad M, Fotuhi-Firuzabad M. On possibilistic and probabilistic uncertainty assessment of power flow problem: A review and a new approach. Renewable and Sustainable Energy Reviews 2014; 37: 883-895.

[32] Ghaemi S, Salehi J, Aghdam FH. Risk aversion energy management in the networked microgrids with presence of renewable generation using decentralised optimisation approach. IET Renewable Power Generation 2018; 13(7): 1050-1061.

[33] Low SH. Convex relaxation of optimal power flow—Part I: Formulations and equivalence. IEEE Transactions on Control Network Systems 2014; 1(1): 15-27.

[34] De Quevedo PM, Contreras J, Rider MJ, Allahdadian J. Contingency assessment and network reconfiguration in distribution grids including wind power and energy storage. IEEE Transactions on Sustainable Energy 2015; 6(4): 1524-1533.